Unconventional dynamic hysteresis in a periodic assembly of paramagnetic colloids

Pietro Tierno,[1,2,*] Tom H. Johansen,[3] and J. M. Sancho[1,2]

[1]*Departament de Estructura i Constituents de la Matèria, Universitat de Barcelona, 08028 Barcelona, Spain*
[2]*Institut de Nanociència i Nanotecnologia, Universitat de Barcelona, 08028 Barcelona, Spain*
[3]*Department of Physics, University of Oslo, P.O. Box 1048, Blindern, Norway*

Dynamic hysteresis phenomena are widespread in physical sciences and describe the complex behavior of systems driven out of equilibrium by a periodic forcing. We use here paramagnetic colloids above a stripe-patterned garnet film as the model system to study dynamic hysteresis, the latter induced when the particles are periodically translated by an oscillating magnetic field. In contrast to the expected behavior for a bistable system, we observe that the area of the hysteresis loop decreases by increasing the driving frequency and reduces to zero for frequencies higher than 5–7 s^{-1}. To explain the experimental results, we develop a simple model based on an overdamped Brownian particle driven by a periodic potential with an oscillating amplitude.

PACS number(s): 82.70.Dd, 75.70.Kw, 75.78.−n

I. INTRODUCTION

The phenomenon of hysteresis is ubiquitous in physical sciences and has been observed in many different scenarios, ranging from ferromagnets [1] to soft materials [2], electronic circuits [3], and biological [4] and optical [5] systems. An overdamped particle driven in a bistable potential, such as a quartic double-well potential, is perhaps the simplest system showing hysteresis and has been frequently invoked to explain the hysteretic behavior of many complex systems. In the absence of any external bias force, the potential has two energy minima separated by a central barrier relatively high with respect to the thermal energy. When a strong bias field is applied, one minimum disappears and the particle is located above the other minimum. If the field is reversed, the roles of the states are interchanged and an irreversible Barkhausen jump of the particle takes place between the two states. If the field is oscillating, driving the particle between these two states, then the order parameter follows a hysteresis loop and its area measures the work dissipated as heat during the whole cycle. During this temporal cycle, the response of the system will depend on the competition between the driving frequency and the internal relaxation of the particle towards the metastable state. In particular, the bistable model predicts that the hysteresis loop area increases with the driving frequency [6], which corresponds to an increase of the amount of energy irreversibly turned into heat. This behavior has been experimentally observed in several works based on ferromagnetic thin films [7–9] and more complex models have been developed [10]. In addition, also different rate-dependent behavior has been experimentally observed where the loop area first increases and then decreases with the driving frequency [11].

In this article, we present experimental results of dynamic hysteresis arising in a magnetic colloidal system. In particular, our system consists of an ensemble of microscale particles magnetically driven above the periodic stripe domain pattern of a uniaxial ferrite garnet film (FGF). An external oscillating magnetic field modulates the magnetic stray field of the FGF in such a way that the particles perform periodic motion between nearest domains. By measuring the particle position relative to these domains, we determine an effective magnetization and construct a dynamic hysteresis loop. We next explore the rate-dependent behavior of the magnetization and find that, in contrast to the bistable system, the area of the hysteresis loop decreases by increasing the driving frequency. To explain this behavior, we introduce a model based on an overdamped Brownian particle driven above a periodic potential with oscillating amplitude. We show that the simple model is able to capture all the main features of the frequency-dependent behavior of the magnetization loops.

II. EXPERIMENT

A. System

In the experiments, we use polystyrene paramagnetic particles with diameter $d = 1.05$ μm and magnetic volume susceptibility $\chi = 1.1$ (Dynabeads Myone). The particles are coated with carboxylic acid groups and stabilized in water at a concentration of $\sim 9 \times 10^9$ beads/mL. We deposit the particles on top of the surface of a uniaxial FGF, which was grown by liquid phase epitaxy on a gadolinium gallium garnet substrate [12]. The FGF was characterized by a spatial periodicity $\lambda = 6.9$ μm and a saturation magnetization $M_s = 1.1 \times 10^4$ A/m.

To induce particle motion from one domain to the next, we apply an oscillating magnetic field in the plane of the film and perpendicular to the magnetic stripes $\boldsymbol{H}(t) \equiv H_0 \sin \omega t \boldsymbol{\hat{e}}_x$, with frequency ω and amplitude H_0. In particular, in most of the experiments we set the amplitude to $H_0 = 800$ A/m and vary the frequency ω and the particle area density $\rho = N/A$, with N the number of particles and A the observation area $A \sim 4500$ μm^2.[1]

---

[1]We found that the amplitude of the magnetic field did not alter the particle dynamics for a field 700 A/m $< H_0 <$ 10 kA/m. For amplitude lower than $H_0 < 700$ A/m, the field was not able to induce the particle motion between nearest domains. In contrast, for amplitude higher than $H_0 > 700$ A/m, we observed that the Bloch

---

*ptierno@ub.edu
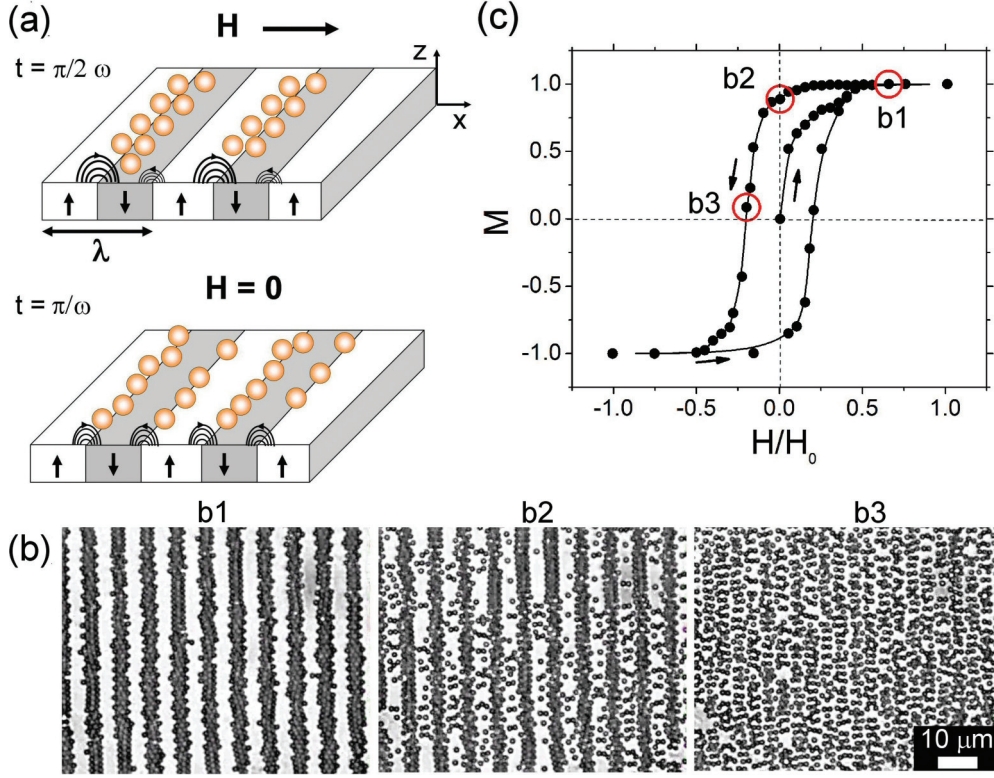
FIG. 1. (Color online) (a) Schematic illustrations of paramagnetic colloids on top of a FGF and subjected to an oscillating magnetic field $\boldsymbol{H}(t) \equiv H_0 \sin{(\omega t)}\hat{\boldsymbol{e}}_x$ at two different times $t = \pi/2\omega$ and π/ω. (b) Three microscope images showing paramagnetic colloids (density $\rho = 0.37 \ \mu\text{m}^{-2}$) above a FGF and subjected to the oscillating field with $\omega = 0.628 \ \text{s}^{-1}$ and $H_0 = 800$ A/m. From left to right, the images were taken at time $t = 4.1$, 4.9, and 5.3 s. (c) Experimental hysteresis loop of the order parameter M versus the applied field H normalized with respect to its amplitude H_0. Red circles denote the corresponding location of the microscope images.

In order to avoid particle sticking to the surface of the FGF, we coat the latter with a 1.7-μm-thick layer of a photoresist (AZ1512, Microchemicals) by using standard spin coating and UV photo-cross-linking [13]. The presence of the polymer coating increases the elevation of the particle center from the surface of the film, reducing the magnetic potential of $\sim$3%.

The external magnetic field was generated by using a computer-controlled Helmholtz coil arranged on the stage of a bright field optical microscope (eclipse NI-U, Nikon) equipped with a CCD camera (Basler 601Fc) working at a temporal resolution of 60 frames per second. Image analysis and tracking routines [14] were used to extract the position of the particles $\{x_i(t)y_i(t)\}$.

B. Results

In Fig. 1(a) we show two schematics illustrating the position of the paramagnetic colloids above the FGF when the applied field is maximal along the $x > 0$ direction ($t = \pi/2\omega$) and is zero ($t = \pi/\omega$). Under a magnetic field $\boldsymbol{H}$, a paramagnetic particle acquires a magnetic moment $\boldsymbol{m} = (\pi/6)d^3\chi\boldsymbol{H}$ pointing along the field direction and its energy is given

by $U = -\mu\boldsymbol{m} \cdot \boldsymbol{H}$, with μ the permeability of the medium. The particles can be moved in a fluid when subjected to a magnetic field gradient since they experience a net force $\boldsymbol{F} = \mu\nabla(\boldsymbol{m} \cdot \boldsymbol{H})$. In particular, as shown in Fig. 1(a), the FGF is characterized by a series of ferromagnetic domains having alternating magnetization with spatial periodicity λ and separated by Bloch walls (BWs), i.e., narrow regions where the magnetic stray field of the film is maximal. Thus, in the absence of an external field, the paramagnetic colloids are attracted by the BWs forming parallel chains with negligible thermal fluctuations and no net motion in the perpendicular direction. We induce particle motion from one domain to the next by applying an in-plane oscillating magnetic field. The field does not change the size of the domains, but it modifies the stray field of the film making stronger (weaker) the BWs, which have magnetic field lines parallel (antiparallel) to the field direction [Fig. 1(b)]. The particles located on a weak wall experience a net magnetic force generated by the gradient between the strong and weak walls and migrate towards the strong walls. In contrast to previous work [15], where a tilted oscillating field was used to create a ratchetlike particle motion, the symmetric modulation prevents any particle flux and the number of particles remains constant within the observation area.

Above a BW, the stray field will induce a magnetic moment $m_i \equiv m(x_i)$ to a paramagnetic colloid i, which points along the direction of the magnetic field line. Thus the moments of the particles arrange in an antiferromagneticlike phase, with spins having opposite orientations each $\lambda/2$. We characterize this

---

walls become distorted by the strong field and the magnetic potential of the film loses its spatial symmetry. As a consequence, it was not possible to measure magnetization from the particle position.

system by introducing an Ising-like magnetization

$$M \equiv \frac{1}{N}\sum_i m_i = \frac{n_p^+ - n_p^-}{N}, \tag{1}$$

where $N = n_p^+ + n_p^-$ and n_p^+ (n_p^-) is the number of particle located on a positive (negative) BW, where the positive (negative) sign is taken with respect to the x axis.

In Fig. 1(c) we plot M for a complete cycle of an applied field oscillating at a frequency $\omega = 0.628$ s^{-1}. Before the field is applied, i.e., in the demagnetized state, the particles are evenly distributed above the film and $M = 0$. When increasing the field, the particles located above a weak BW start moving towards the nearest strong BW, increasing the density of the chains above this BW. During the first half cycle, the magnetization rises towards a saturation state, showing a steep virgin curve. In the saturated state, all BWs of weak polarity are completely depleted of particles, while dense aggregates are formed above the strong BWs. Lowering the field releases some particles from these aggregates, but even for $H_0 = 0$ the system retains a considerable degree of magnetization $M = 0.89$. At the coercive field of $H_0 \sim 160$ A/m, the magnetization becomes zero and all particles distribute evenly above the film [Fig. 1(b3)]. For fixed frequency and field strength, the magnetization curve features the same shape, even after several field cycles.

We next characterize the rate-dependent behavior of the order parameter M and perform a series of full-cycle experiments at different frequencies of the applied field and particle area density. Figures 2(a) and 2(b) show results of such measurements for two different area densities. In both cases, we find that the area of the hysteresis loop decreases with increasing frequency and for values higher than 5–7 s^{-1}, the system behavior becomes essentially reversible. Increasing further the frequency, this type of behavior persists up to values $\omega \sim 900$ s^{-1}; above this value, we find that the particles are unable to follow the fast vibration of the potential. In contrast, for lower frequencies, the area increases until the loop becomes a complete square for $\omega \sim 7 \times 10^{-4}$ s^{-1}.

The fact that the behavior of the magnetization did not change significantly with the particle density makes evident the negligible role of the interparticle interactions compared to the interaction with the substrate. At low area density, most of the particles are seen to move from one BW to the next one with no collision, showing a straight periodic trajectory perpendicular to the stripe pattern and slightly perturbed in the lateral direction by small thermal fluctuations. Increasing the density enforces the collision between the particles during their periodic excursions. In the saturation state, the particles tend to form parallel chains stacked together as a consequence of particle jamming [16]. At high area density, the frequent collisions between the particles increase the effective temperature of the bath, but we find that this does not affect the magnetization dynamics significantly.

III. MODEL

We model the dynamics of a paramagnetic colloid above the FGF as an overdamped Brownian particle subjected to a periodic potential $V(X,t)$, where $X \equiv x/\lambda$. The corresponding
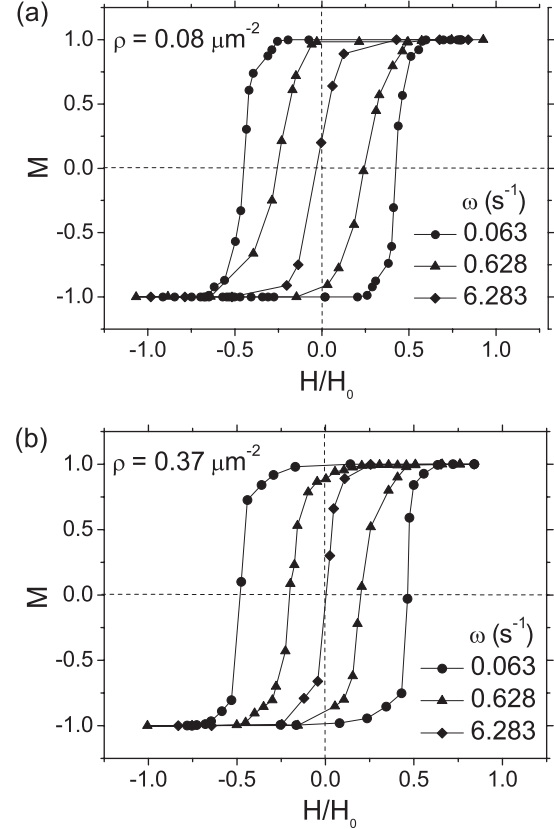

FIG. 2. Experimental hysteresis loops showing the variation of M versus the applied field H normalized with respect to its amplitude H_0 at different frequencies. The particle density used are (a) $\rho = 0.08$ μm^{-2} and (b) $\rho = 0.37$ μm^{-2}.

one-dimensional (1D) Langevin equation has the form

$$\gamma \dot{X} = -V'(X,t) + \sqrt{2k_B T \gamma}\,\xi(t), \tag{2}$$

where γ is the effective friction of the medium and $\xi(t)$ represents Gaussian white noise with zero mean and δ correlated. The magnetic potential above the surface of the FGF has a complex form and has been analytically derived in Ref. [15] In the present case, we verified that the potential seen by one particle can be mapped into a simpler expression

$$V(X,t) = V_0[\cos(\omega t)\cos(2\pi X) + A\cos(4\pi X)]. \tag{3}$$

Here the second term in Eq. (3) ensures the periodicity of the film at zero applied field with very small energetic barriers between the wells, of height A. Then Eq. (2) reduces to

$$\dot{X} = -\frac{2\pi V_0}{\gamma}[\cos(\omega t)\sin(2\pi X) + 2A\sin(4\pi X)]$$
$$+ \sqrt{2D}\,\xi(t),$$

where $D = k_B T/\gamma$ is the particle diffusion coefficient. A similar stochastic differential equation has been already described in recent works [17], which focus on the effect of an added bias force.

It follows from Eq. (3) that the particle dynamics is governed by two time scales: the period of the driving field $T = 2\pi/\omega$ and the relaxation time τ_r, which is the time

required for the particle to move from one potential maximum to the next stable one. For frequencies $\omega \gg 1/\tau_r$ the variation of the potential is too fast and after a short transient, the particle performs localized oscillations around the same potential minimum. When $\omega \leqslant 1/\tau_r$, the particle has time to pass from one minimum to the next one and thus to explore larger regions of the potential landscape.

To simulate Eq. (4) we use the parameters $V_0 \sim \mu V \chi H_0^2 = 1.4 \times 10^{-3}$ J/m and $\gamma = 2.7 \times 10^{-3}$ Pa s, where all lengths have been normalized by λ. We use a stochastic Runge-Kutta algorithm [18] for $N = 1000$ noninteracting particles with initial random location and an integration time step of $dt = 10^{-3}$. Initially, the particles were distributed randomly along a segment of length 3λ and with periodic boundary conditions at its ends. We divide this segment in six equal regions that correspond to the alternating signs of the BWs and assign to each particle a sign depending on its location above this segment. Finally, we measure the system magnetization following Eq. (1).

Some representative results of these simulations are shown in Fig. 3(a) . The hysteresis loops obtained from the model
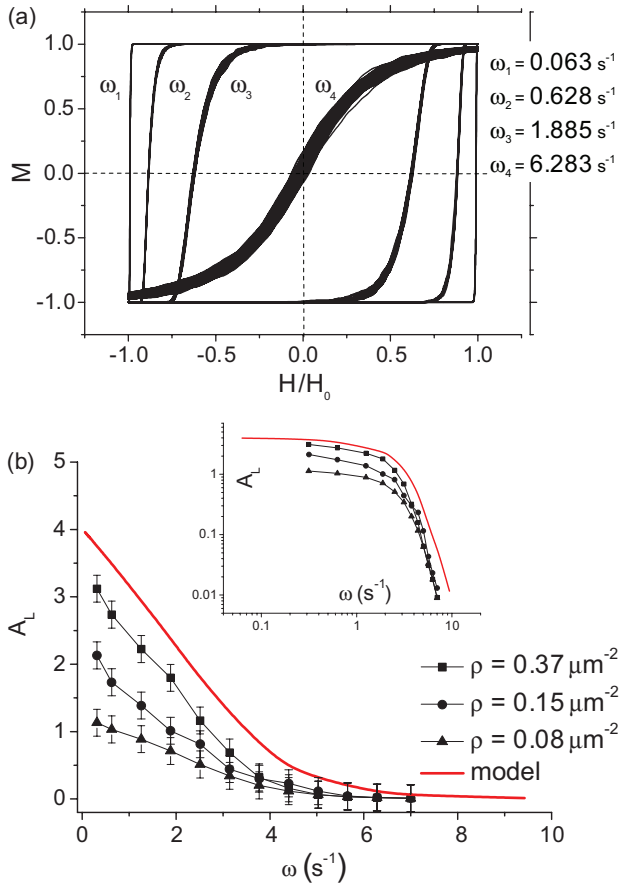

FIG. 3. (Color online) (a) Hysteresis loops obtained from numerical simulations at four different frequencies. As the effective diffusion coefficient of the particles we use $D/\lambda = 0.1 \times 10^{-3}$ μm/s and set $A = 0.1 \times 10^{-2}$. The rest of the parameters are the same as the experimental ones. (b) Comparison between the experimental (point) and theoretical (red line) hysteresis loop area A_L versus driving frequency ω. The inset shows the same graph on a double logarithmic scale.

show the same overall rate-dependent behavior as the experimental ones and in both cases the area of the loops becomes zero for frequencies higher than $\omega \sim 5$–7 s^{-1}. To better compare the model with the experimental data, we plot in Fig. 3(b) the loop area $A_L = \oint M(H)dH$ as a function of frequency for three different area densities and show as a continuous line the values obtained from the simulation. In particular, we find that the model departs from the experiments in the low-frequency regime, while at high frequencies, all curves tend to merge into a single one. The failure of our model to capture the behavior at low frequencies can be attributed either to the absence of interparticle interactions, such as magnetic or electrostatic ones, or to its 1D nature, in contrast to the real particle motion occurring in two dimensions. However, despite these limitations, it allows us to capture the main physical behavior displayed by this colloidal system.

IV. CONCLUSION

We showed that an ensemble of paramagnetic colloids above a stripe-patterned magnetic garnet film can be used as a model system to study dynamic hysteresis phenomena. In particular, we found that the observed dynamics is not related to a Barkhausen jump between the states and the area of the magnetization curve decreases with increasing driving frequency, which is the opposite behavior of bistable systems. We explained this unconventional dynamics by using a simple model of a periodic potential with an oscillating amplitude. Due to the accessible length and time scale of colloidal particles, the presented system introduces a way to study the effect of periodic forcing on collective particle organization with single-particle resolution.

APPENDIX: LANDAU MODEL

The most common hysteresis phenomena can be explained by using the Landau potential

$$V(x,t) = V_0 \left(-\frac{x^2}{2} + \frac{x^4}{4} \right) + H_0 x \cos(\omega t) \qquad (A1)$$

placed in the Langevin equation (2) for an overdamped Brownian particle. The potential in Eq. (A1) is the Landau energy plus an oscillating field.

Let us consider an ensemble of independent particles subjected to this type of potential. For times t_i such that $\cos(\omega t_i) \sim 0$, the system presents two coexisting stable states separated by a large energy barrier $\Delta V = V_0/4 \gg k_B T$. In this temporal regime, the time scale of the particles relaxing towards the other steady state is very small and the particles are unable to follow the change of sign of the potential and

as a consequence the hysteresis cycle appears. At higher frequencies this effect become more pronounced and the area of the hysteresis loop increases.

In contrast to the Landau potential, the energetic barrier in the potential (3) when the system is in the bistable regime $[\cos(\omega t_i) \sim 0]$ is much smaller and thus the particles disperse more evenly above the film. Both phenomena can be also interpreted in the different evolution of the density of particles near the coexistence region where the differences between the time scales are relevant.

---

[1] G. Bertotti, *Hysteresis in Magnetism: For Physicists, Materials Scientists, and Engineers* (Academic, San Diego, 1998); B. K. Chakrabarti and M. Acharyya, Rev. Mod. Phys. **71**, 847 (1999).

[2] L. B. Chen, C. F. Zukoski, B. J. Ackerson, H. J. M. Hanley, G. C. Straty, J. Barker, and C. J. Glinka, Phys. Rev. Lett. **69**, 688 (1992); F. Da Cruz, F. Chevoir, D. Bonn, and P. Coussot, Phys. Rev. E **66**, 051305 (2002); J. Mewis and N. J. Wagner, J. Colloid Interface Sci. **147–148**, 214 (2009).

[3] O. H. Schmitt, J. Sci. Instrum. **15**, 24 (1938).

[4] D. Williams, G. Phillips, and R. Sekuler, Nature (London) **324**, 253 (1986); J. R. Pomerening, E. D. Sontag, and J. E. Ferrell, Jr., Nat. Cell Biol. **5**, 346 (2003).

[5] H. M. Gibbs, *Optical Bistability: Controlling Light with Light* (Academic, Orlando, 1985); R. Bonifacio and L. A. Lugiato, Phys. Rev. Lett. **40**, 1538 (1978).

[6] P. Jung, G. Gray, R. Roy, and P. Mandel, Phys. Rev. Lett. **65**, 1873 (1990).

[7] C. Appino, G. Bertotti, O. Bottauscio, M. Chiampi, F. Fiorillo, M. Repetto, and P. Tiberto, J. Appl. Phys. **79**, 4575 (1996); V. Basso, G. Bertotti, O. Bottauscio, F. Fiorillo, M. Pasquale, M. Chiampi, and M. Repetto, *ibid.* **81**, 5606 (1997).

[8] J.-S. Suen and J. L. Erskine, Phys. Rev. Lett. **78**, 3567 (1997).

[9] B. C. Choi, W. Y. Lee, A. Samad, and J. A. C. Bland, Phys. Rev. B **60**, 11906 (1999).

[10] M. Rao, H. R. Krishnamurthy, and R. Pandit, Phys. Rev. B **42**, 856 (1990); C. N. Luse and A. Zangwill, Phys. Rev. E **50**, 224 (1994); M. C. Mahato and S. R. Shenoy, *ibid.* **50**, 2503 (1994); S. W. Sides, P. A. Rikvold, and M. A. Novotny, Phys. Rev. Lett. **81**, 834 (1998); M. A. Pustovoit, A. M. Berezhkovskii, and S. M. Bezrukov, J. Chem. Phys. **125**, 194907 (2006); B. Dybiec and E. Gudowska-Nowak, J. Stat. Mech. (2009) P05004.

[11] Y.-L. He and G.-C. Wang, Phys. Rev. Lett. **70**, 2336 (1993); L. Laurson and M. J. Alava, *ibid.* **109**, 155504 (2012); M. Das, D. Mondal, and D. S. Ray, J. Chem. Phys. **136**, 114104 (2012).

[12] L. E. Helseth, T. Backus, T. H. Johansen, and T. M. Fischer, Langmuir **21**, 7518 (2005); P. Tierno, F. Sagués, T. H. Johansen, and T. M. Fischer, Phys. Chem. Chem. Phys. **11**, 9615 (2009).

[13] P. Tierno, Phys. Rev. Lett. **109**, 198304 (2012).

[14] J. C. Crocker and D. G. Grier, J. Colloid Interface Sci. **179**, 298 (1996).

[15] P. Tierno, S. V. Reddy, T. H. Johansen, and T. M. Fischer, Phys. Rev. E **75**, 041404 (2007); P. Tierno, S. V. Reddy, M. G. Roper, T. H. Johansen, and T. M. Fischer, J. Phys. Chem. B **112**, 3833 (2008).

[16] L. E. Helseth, H. Z. Wen, T. M. Fischer, and T. H. Johansen, Phys. Rev. E **68**, 011402 (2003).

[17] P. Romanczuk, F. Müller, and L. Schimansky-Geier, Phys. Rev. E **81**, 061120 (2010); Stoch. Dynam. **11**, 461 (2011).

[18] R. L. Honeycutt, Phys. Rev. A **45**, 600 (1992).